

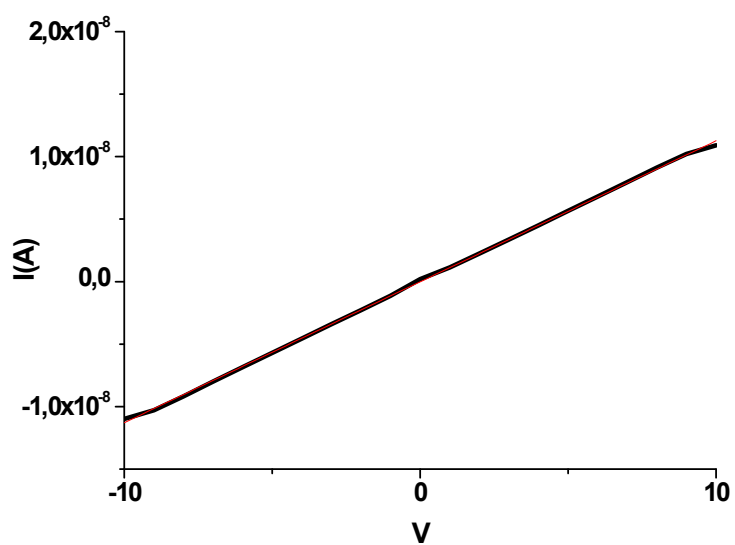
## **Supplementary Information**

Reversible Recrystallization Process of Copper and Silver Thioacetamide-Halide Coordination Polymers and their Basic Building Blocks

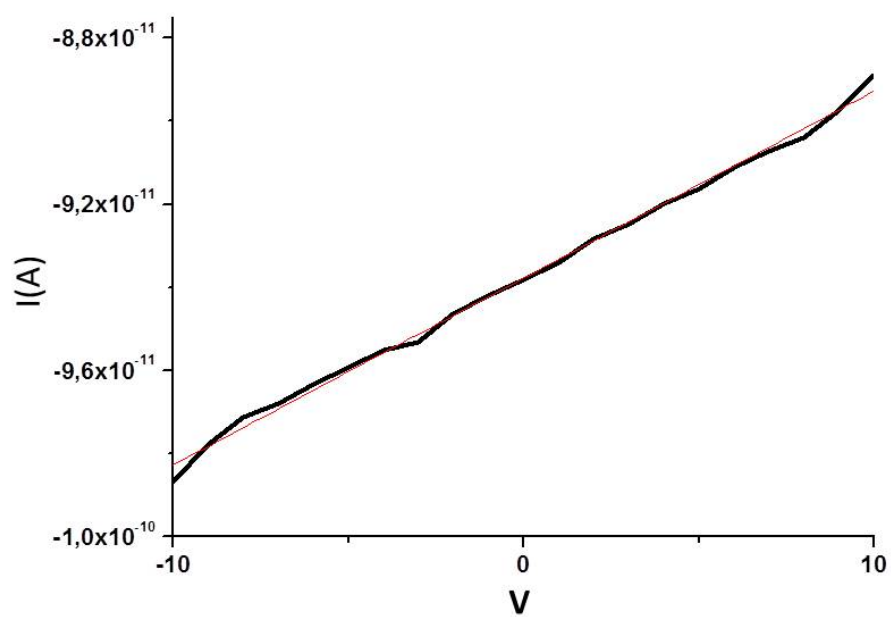
J. Troyano, J. Perles, P. Amo-Ochoa, J. I. Martínez, F. Zamora,\* and S. Delgado\*

Table S1. Crystal and refinement data for **1-4**.

	1	2	3	4
<b>Chemical formula</b>	C <sub>2</sub> H <sub>3</sub> BrCuNS	C <sub>2</sub> H <sub>3</sub> CuINS	C <sub>2</sub> H <sub>3</sub> AgCINS	C <sub>2</sub> H <sub>3</sub> AgBrNS
<b>Formula weight</b>	218.58	265.57	218.45	262.91
<b>Temperature</b>	296(2) K	296(2) K	296(2) K	296(2) K
<b>Wavelength</b>	0.71073 Å	0.71073 Å	0.71073 Å	0.71073 Å
<b>Crystal size</b>	0.28 x 0.32 x 0.33 mm	0.12 x 0.13 x 0.21 mm	0.01 x 0.09 x 0.18 mm	0.08 x 0.12 x 0.14 mm
<b>Crystal habit</b>	clear pale yellow hexagonal prism	clear colourless hexagonal prism	clear light bronze plate	clear pale yellow prismatic
<b>Crystal system</b>	trigonal	trigonal	orthorhombic	orthorhombic
<b>Space group</b>	<i>P</i> 3c1	<i>P</i> 31c	<i>Pbcm</i>	<i>Pbcm</i>
<b>Unit cell dimensions</b>	a = 19.9588(8) Å b = 19.9588(8) Å c = 7.6768(4) Å	a = 11.7896(2) Å b = 11.7896(2) Å c = 8.15090(10) Å	a = 8.8371(3) Å b = 8.4068(2) Å c = 7.4343(2) Å	a = 8.9917(2) Å b = 8.4982(2) Å c = 7.7639(2) Å
<b>Volume</b>	2648.4(2) Å <sup>3</sup>	981.15(3) Å <sup>3</sup>	552.31(3) Å <sup>3</sup>	593.26(2) Å <sup>3</sup>
<b>Z</b>	18	6	4	4
<b>Density (calculated)</b>	2.467 Mg/cm <sup>3</sup>	2.697 Mg/cm <sup>3</sup>	2.627 Mg/cm <sup>3</sup>	2.944 Mg/cm <sup>3</sup>
<b>Absorption coefficient</b>	10.710 mm <sup>-1</sup>	8.248 mm <sup>-1</sup>	4.357 mm <sup>-1</sup>	10.341 mm <sup>-1</sup>
<b>F(000)</b>	1872	732	416	488
<b>Theta range for data collection</b>	2.04 to 25.35°	1.99 to 38.78°	3.34 to 25.32°	3.30 to 27.47°
<b>Index ranges</b>	-21 ≤ h ≤ 24, -24 ≤ k ≤ 24, -9 ≤ l ≤ 9	-20 ≤ h ≤ 20, -20 ≤ k ≤ 18, -14 ≤ l ≤ 14	-10 ≤ h ≤ 10, -10 ≤ k ≤ 10, -8 ≤ l ≤ 8	-11 ≤ h ≤ 11, -10 ≤ k ≤ 11, -10 ≤ l ≤ 10
<b>Reflections collected</b>	38957	28499	6752	6569
<b>Independent reflections</b>	3245 [R(int) = 0.0461]	3744 [R(int) = 0.0463]	549 [R(int) = 0.0404]	1336 [R(int) = 0.0404]
<b>Coverage of independent reflections</b>	99.9%	99.9%	99.8%	99.9%
<b>Absorption correction</b>	multi-scan	multi-scan	multi-scan	multi-scan
<b>Max. and min. transmission</b>	0.1534 and 0.1261	0.4377 and 0.2762	0.9577 and 0.5077	0.4917 and 0.3254
<b>Data / restraints / parameters</b>	3245 / 25 / 177	3744 / 1 / 57	549 / 0 / 37	726 / 0 / 37
<b>Goodness-of-fit on F<sup>2</sup></b>	1.003	1.005	1.000	1.000
<b>Final R indices</b> I > 2σ(I) all data	R1 = 0.0295, wR2 = 0.0842 R1 = 0.0412, wR2 = 0.1004	R1 = 0.0311, wR2 = 0.0862 R1 = 0.0605, wR2 = 0.1109	R1 = 0.0296, wR2 = 0.0720 R1 = 0.0391, wR2 = 0.0785	R1 = 0.0285, wR2 = 0.0738 R1 = 0.0345, wR2 = 0.0767
<b>Absolute structure parameter</b>	0.0(0)	0.0(0)		
<b>Largest diff. peak and hole</b>	1.123 and -0.696 eÅ <sup>-3</sup>	0.965 and -0.857 eÅ <sup>-3</sup>	1.216 and -0.914 eÅ <sup>-3</sup>	0.936 and -1.244 eÅ <sup>-3</sup>
<b>R.M.S. deviation from mean</b>	0.204 eÅ <sup>-3</sup>	0.195 eÅ <sup>-3</sup>	0.119 eÅ <sup>-3</sup>	0.151 eÅ <sup>-3</sup>



**Figure S1.** Intensity versus voltage obtained for a crystal of  $[\text{CuBr}(\text{TAA})]_n$  (1).



**Figure S2.** Intensity versus voltage obtained for a crystal of  $[\text{CuI}(\text{TAA})]_n$  (2).

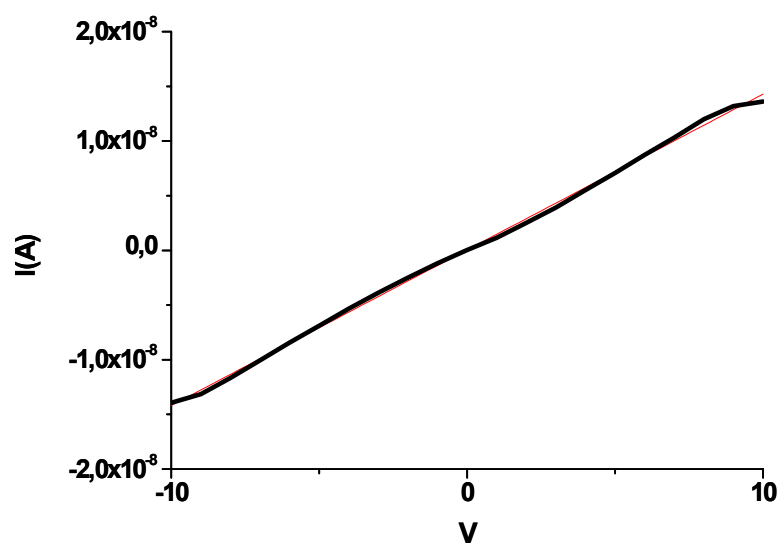


**Figure S3.** Intensity versus voltage obtained for a crystal of  $[\text{AgCl}(\text{TAA})]_n$  (3).

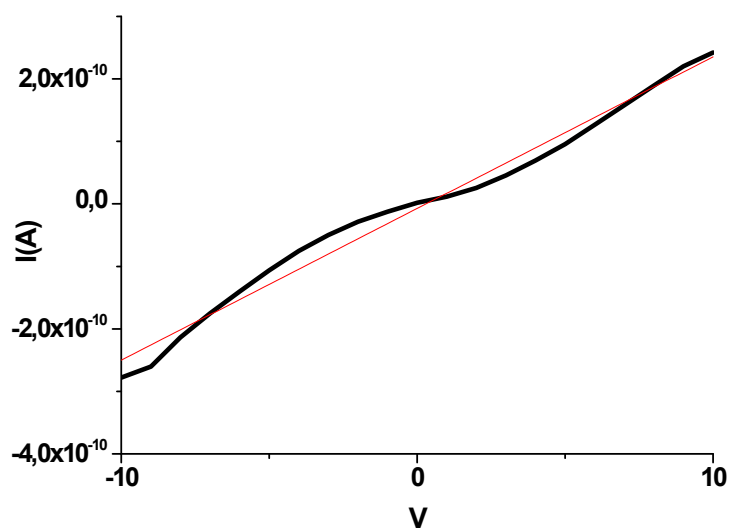


**Figure S4.** Intensity versus voltage obtained for a crystal of  $[\text{AgBr}(\text{TAA})]_n$  (4).

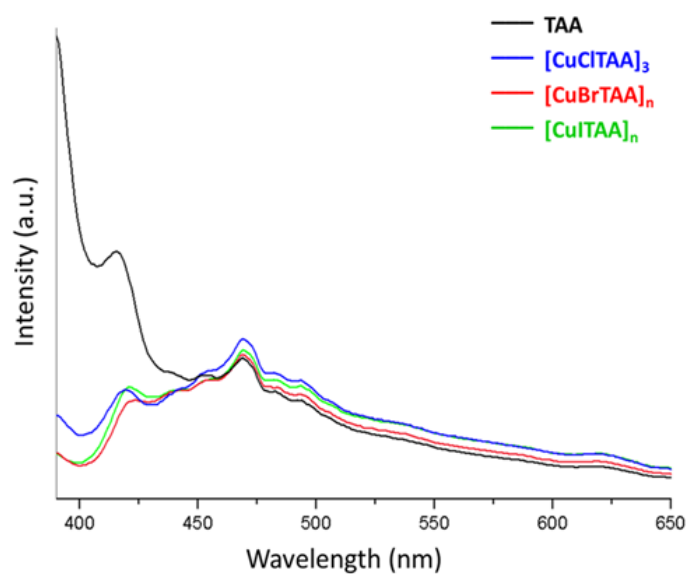


**Figure S5.** Emission spectra of TAA and  $[\text{CuX}(\text{TAA})]_n$  compounds ( $\text{X} = \text{Cl}$ , Br(1), I (2)) in the solid state at 359 nm.

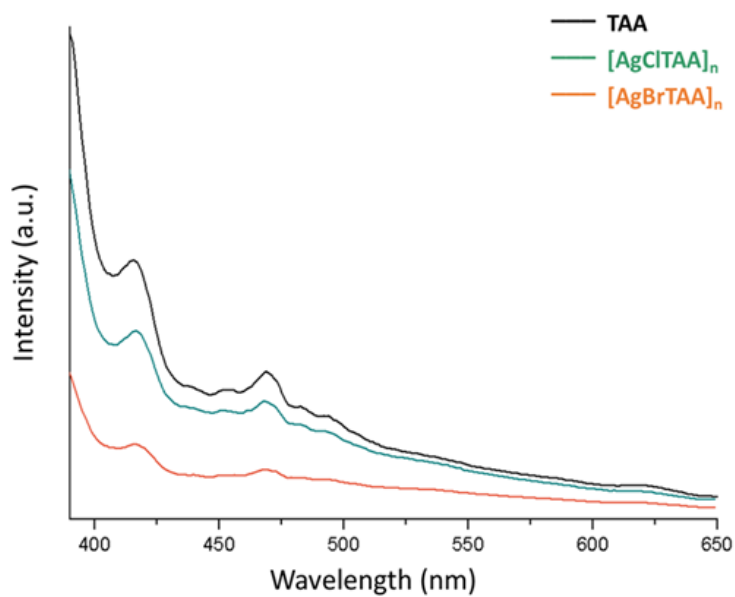


**Figure S6.** Emission spectra of TAA and  $[\text{AgXTAA}]_n$  compounds [ $\text{X} = \text{Cl}$  (3), Br (4)] in the solid state at 359 nm.

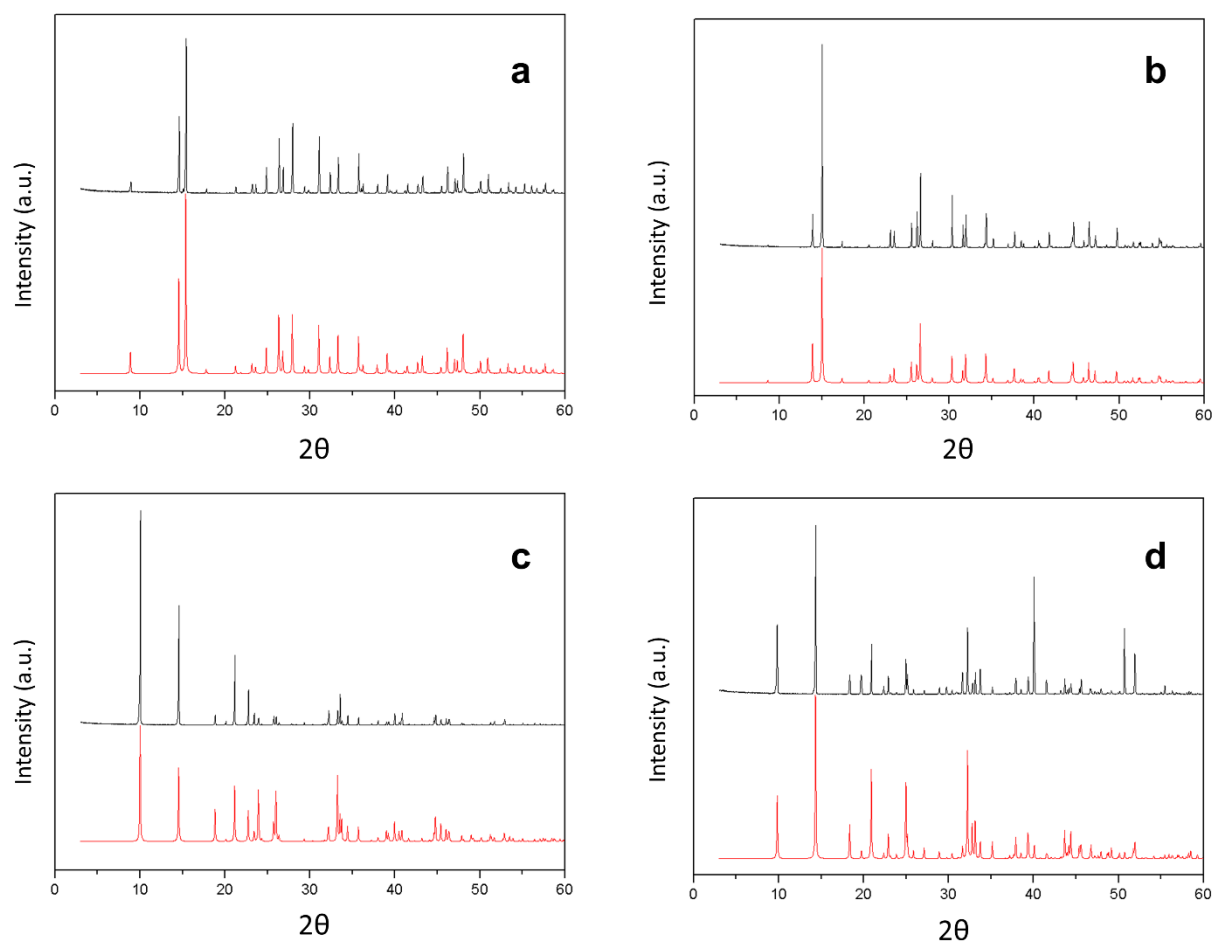


**Figure S7.** XRPD pattern of **1** (a), **2** (b), **3** (c) and **4** (d). Experimental (*black*) and simulated (*red*).

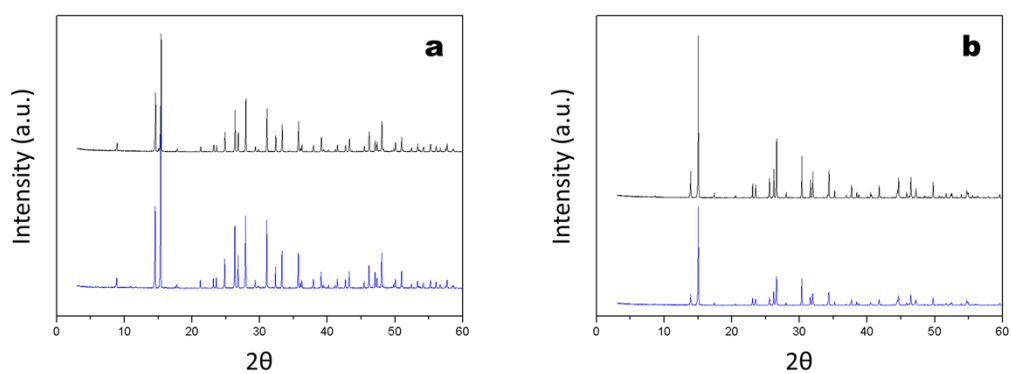


**Figure S8.** XRPD pattern of **1** (a) and **2** (b) before dissolving in acetonitrile (black) and after extracting the solvent (blue).

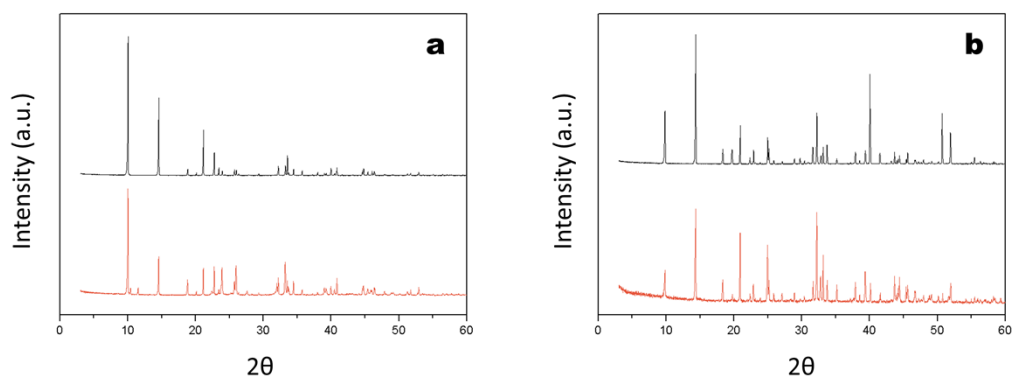


**Figure S9.** XRPD pattern of **3** (a) and **4** (b) before dissolving in pyridine (black) and after extracting the solvent (red).

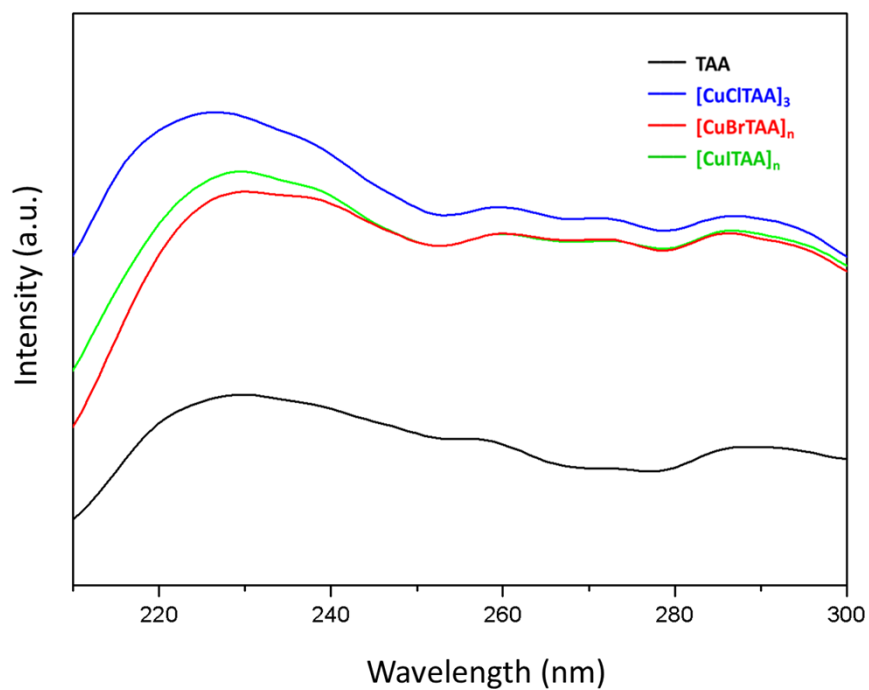


**Figure S10.** UV-vis diffuse reflectance of thioacetamide (TAA) and  $[\text{CuXTAA}]$  ( $\text{X} = \text{Cl}, \text{Br}, \text{I}$ ) compounds at room temperature.

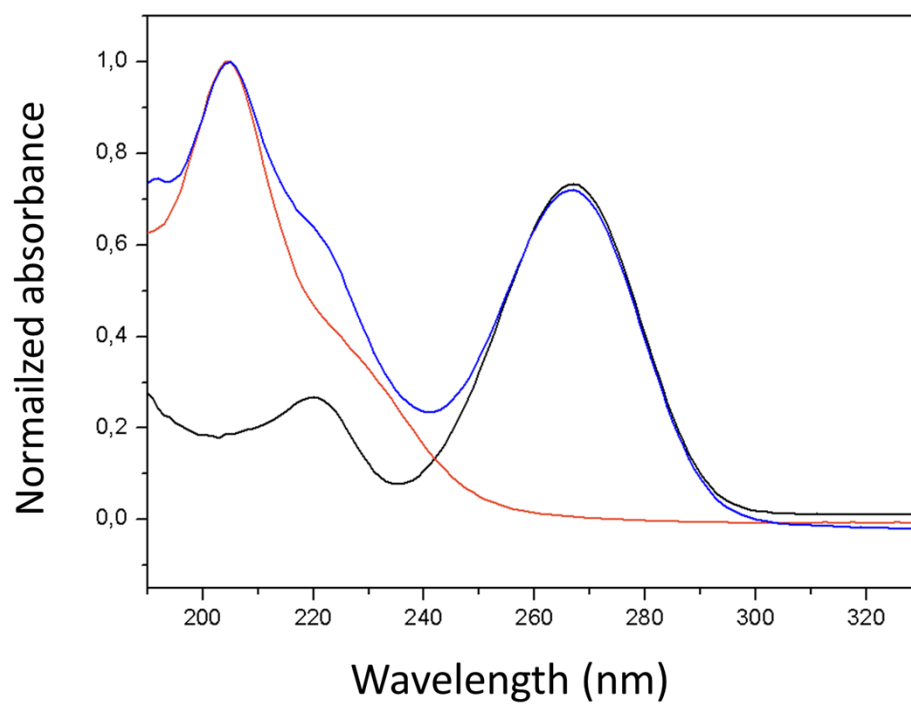


**Figure S11.** UV-vis in acetonitrile solution of  $[\text{CuClTAA}]_3$  (blue), TAA (black) and CuCl (orange).

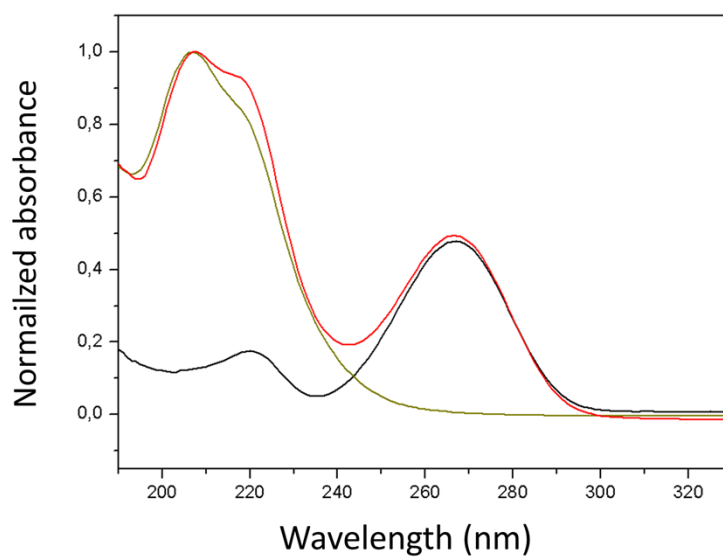


**Figure S12.** UV-vis in acetonitrile solution of  $[\text{CuBrTAA}]_n$  (1) (red), TAA (black) and CuBr (dark yellow).



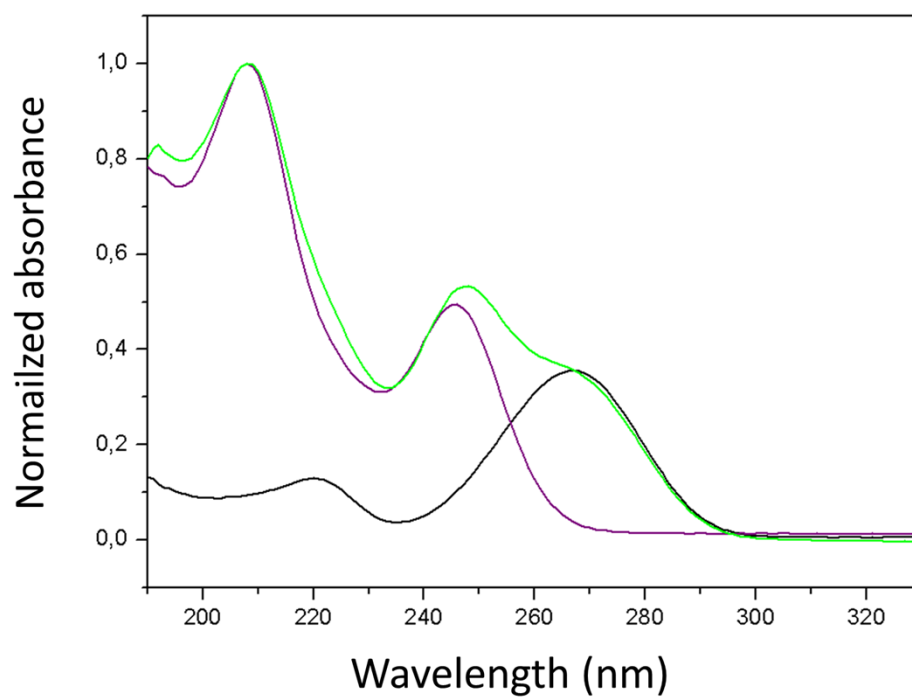


**Figure S13.** UV-vis in acetonitrile solution of  $[\text{CuITAA}]_n$  (**2**) (green), TAA (black) and CuI (purple).

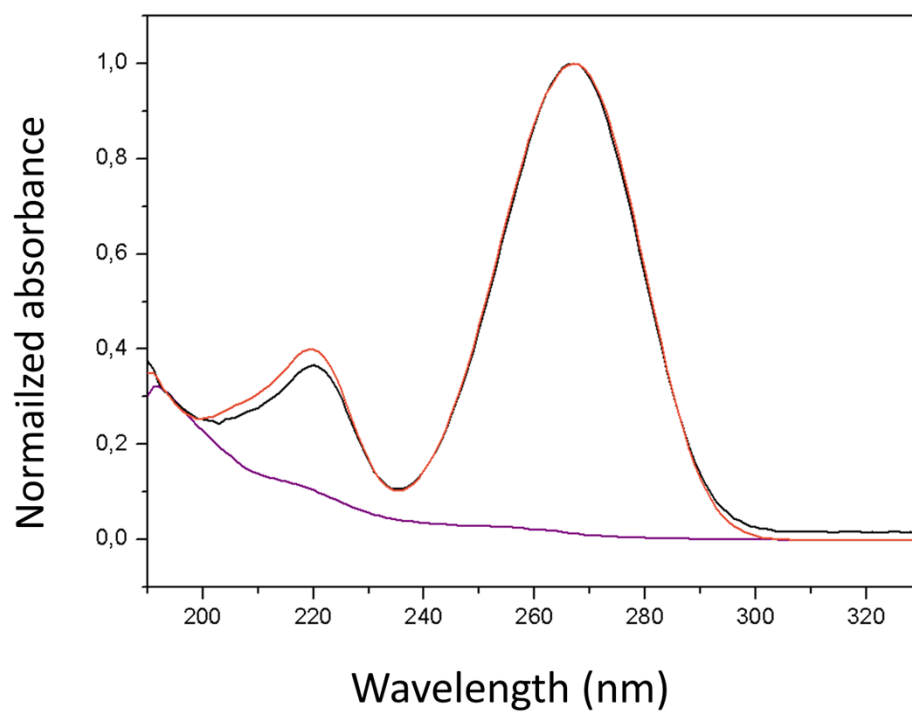


**Figure S14.** UV-vis in acetonitrile solution of  $[\text{AgCITAA}]_n$  (**3**) (orange), TAA (black) and AgCl (purple).

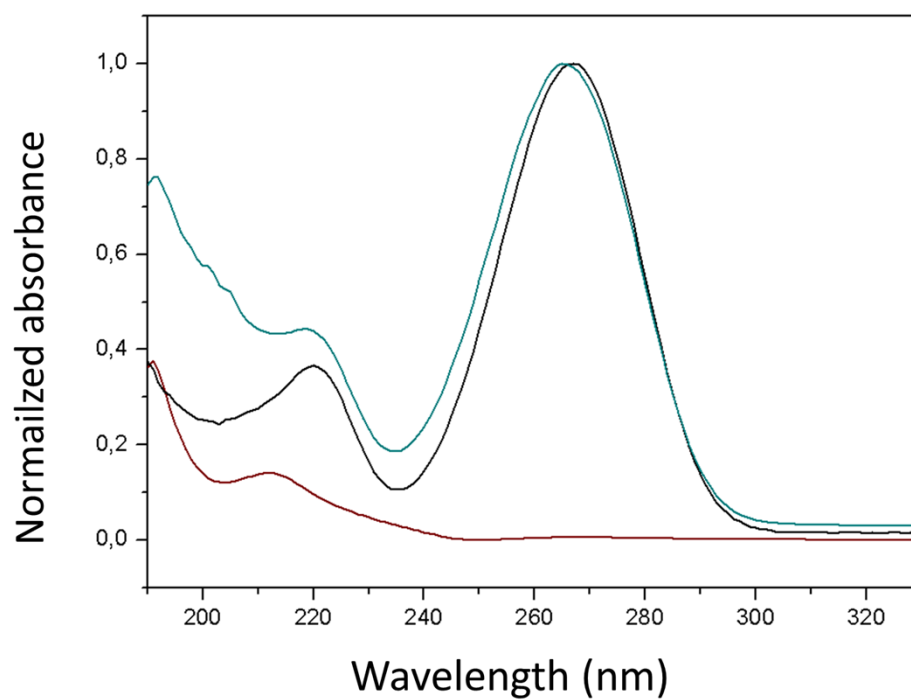


**Figure S15.** UV-vis in acetonitrile solution of  $[\text{AgBrTAA}]_n$  (**4**) (green), TAA (black) and AgBr (dark red).

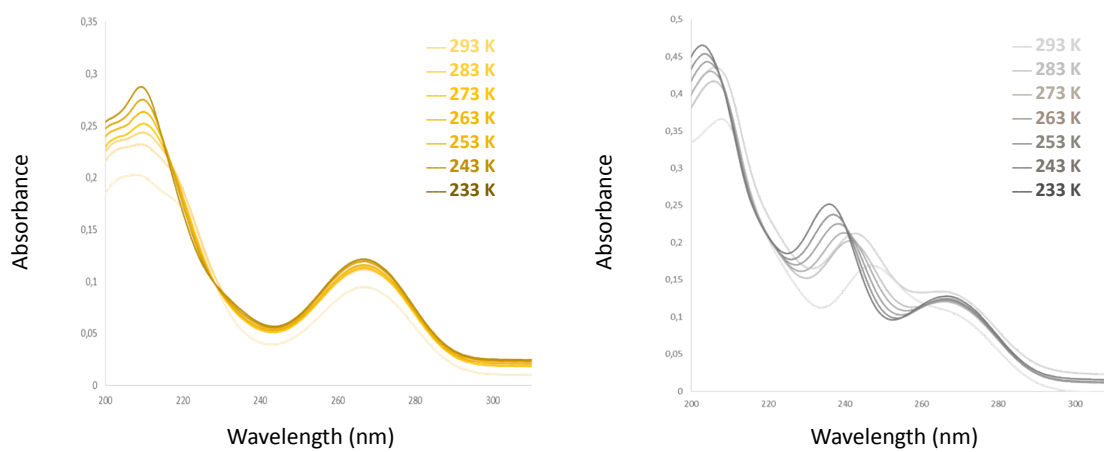


**Figure S16.** UV-vis absorption spectra for **1** (yellow) and **2** (grey) at variable temperature.

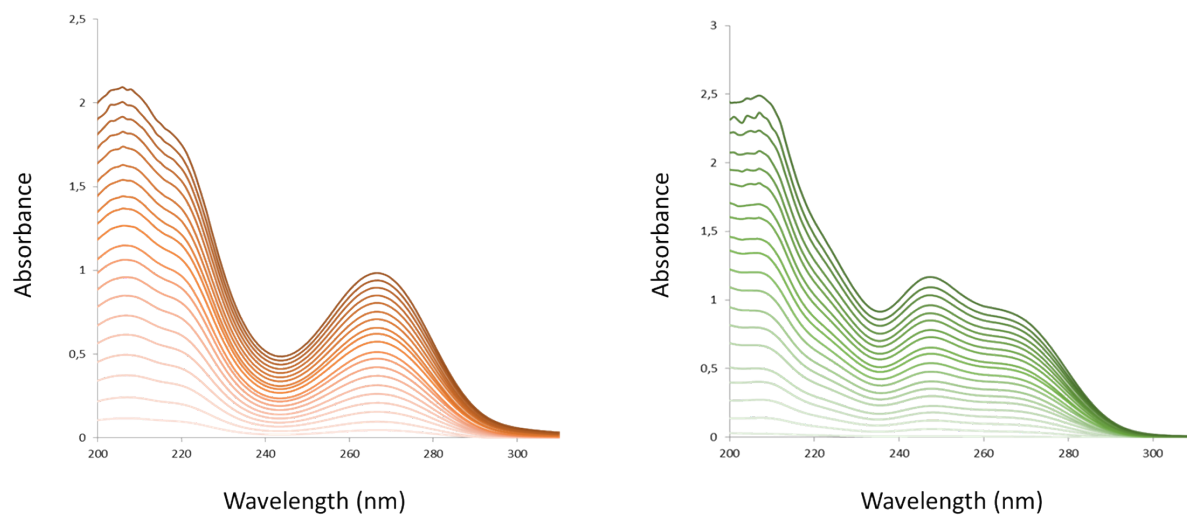


**Figure S17.** Concentration dependence ( $10^{-4}$  to  $10^{-6}$  mol·L $^{-1}$ ) UV-vis absorption spectra for **1** (red) and **2** (green).

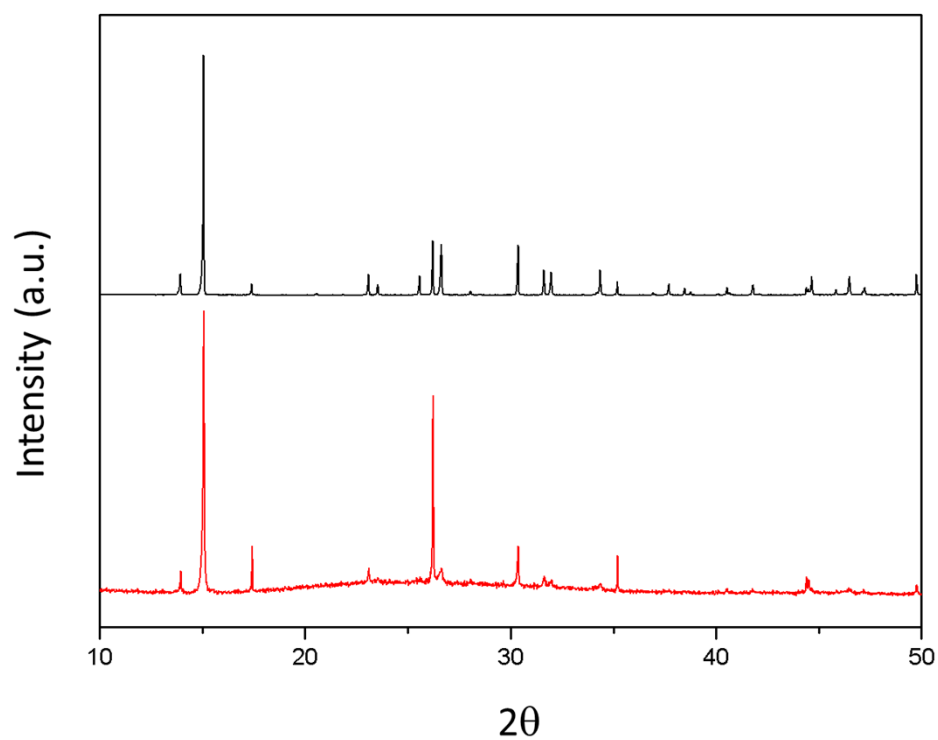


**Figure S18.** XRPD pattern of **2** (black) and thin film obtained by drop-casting a acetonitrile solution of **2** on glass (red).

## THEORETICAL CALCULATIONS

In order to shed some light on the electronic structure properties of the three-dimensional  $[\text{CuX}(\text{TAA})]_n$  ( $\text{X}=\text{Br}$  (1),  $\text{I}$  (2)) and bi-dimensional  $[\text{AgX}(\text{TAA})]_n$  ( $\text{X}=\text{Cl}$  (3),  $\text{Br}$  (4)) coordination polymers, we have carried out accurate Density Functional Theory (DFT)-based calculations by using the efficient plane-wave code PWSCF.<sup>1</sup> In this atomistic simulation package the Kohn-Sham equations are solved using a periodic supercell geometry. The ion-electron interaction is modeled by ultrasoft pseudopotentials<sup>2</sup> and exchange-correlation (XC) effects are treated by the generalized-gradient-approximation (GGA) of Perdew, Burke, and Ernzerhof (PBE).<sup>3</sup> The one-electron wave-functions are expanded in a basis of plane-waves with energy cut-offs of 400 and 500 eV for the kinetic energy and for the electronic density, respectively, which have been adjusted to achieve sufficient accuracy in the total energy. The Brillouin zones of the different bulk-systems were sampled by using  $[2 \times 2 \times 4]$  and  $[3 \times 3 \times 4]$  Monkhorst-Pack grids<sup>4</sup> for the  $[\text{CuBr}(\text{TAA})]_n$  and  $[\text{CuI}(\text{TAA})]_n$ , respectively, and  $[4 \times 4 \times 4]$  Monkhorst-Pack grids for both  $[\text{AgCl}(\text{TAA})]_n$  and  $[\text{AgBr}(\text{TAA})]_n$ .

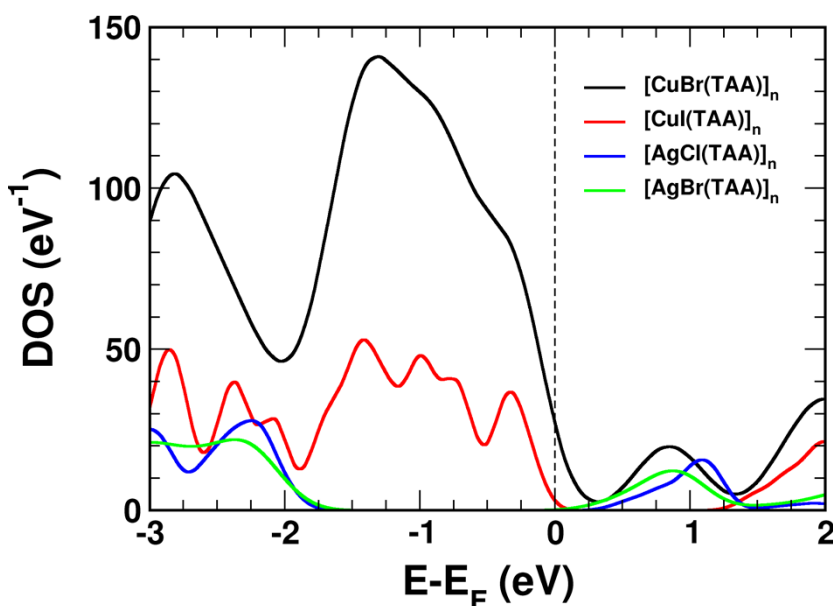


**Figure S19.** Calculated density of electronic states (in  $\text{eV}^{-1}$ ) for the  $[\text{CuBr}(\text{TAA})]_n$ ,  $[\text{CuI}(\text{TAA})]_n$ ,  $[\text{AgBr}(\text{TAA})]_n$  and  $[\text{AgCl}(\text{TAA})]_n$  coordination polymers as a function of the energy, referred to the Fermi level. Each energy level has been broadened with by a Lorentzian profile with a line-width of 0.1 eV.

## **References**

- <sup>1</sup> P. Giannozzi, *et al.*, *J. Phys. Condens. Matter* **21**, 395502 (2009); [www.quantum-espresso.org](http://www.quantum-espresso.org).
- <sup>2</sup> D. Vanderbilt, *Phys. Rev. B* **41**, 7892 (1990).
- <sup>3</sup> J. P. Perdew, K. Burke, M. Ernzerhof, *Phys. Rev. Lett.* **77**, 3865 (1996).
- <sup>4</sup> D. J. Chadi, M. L. Cohen, *Phys. Rev. B* **8**, 5747 (1973).